Zoosyst. Evol. 101 (3) 2025, 999–1012 | DOI 10.3897/zse.101.140898

PENSOFT

MUSEUM FÜR NATURKUNDE BERLIN

Three new species of *Neodon* (Rodentia, Cricetidae) from Sichuan and Xizang, China

Xuming Wang[1], Xuan Pan[2], Yingxun Liu[1,3], Robert W. Murphy[4], Buqing Peng[1], Chao Duan[1,5], Rui Liao[1], Xin Wang[1], Shaoying Liu[1]

1 *Sichuan Academy of Forestry, Ecological Restoration and Conservation for Forest and Wetland Key Laboratory of Sichuan Province, 610081, Chengdu, Sichuan, China*

2 *Chengdu Institute of Biology, Chinese Academy of Sciences, 610213, Chengdu, Sichuan, China*

3 *Sichuan Center for Disease Control and Prevention, 610044, Chengdu, Sichuan, China*

4 *Department of Natural History, Royal Ontario Museum, 100 Queens Park, Toronto, Ontario, M5S 2C6, Canada*

5 *Key Laboratory of Bio-Resource and Eco-Environment of Ministry of Education, Sichuan Key Laboratory of Conservation Biology on Endangered Wildlife, College of Life Science, Sichuan University, 610065, Chengdu, Sichuan, China*

https://zoobank.org/96D25BEE-0A2E-4456-98E4-C32530D74839

Corresponding author: Shaoying Liu (shaoyliu@163.com)

Academic editor: Melissa T. R. Hawkins ♦ **Received** 3 November 2024 ♦ **Accepted** 15 April 2025 ♦ **Published** 28 May 2025

Abstract

During a survey of small mammals in Sichuan and southern Xizang, China, three species of *Neodon* were collected that did not match to any described species. Therefore, we conducted phylogenetic analyses of the entire genus based on two mitochondrial genes (*CYTB* and *ND2*) and three nuclear genes (*IRBP*, *GHR*, and *RAG1*). Morphological analyses were based on skull characteristics and male genitalia. The main results were as follows: 1) Three new taxa consistently formed three distinct clades in the molecular phylogenetic trees; 2) the Kimura 2-Parameter (K2P) distances between these three new taxa and other known species of *Neodon* ranged from 9.0% to 15.5%, indicating interspecific divergence; 3) both automatic barcode gap discovery (ABGD) and Bayesian posterior probability (BPP) analyses indicated that the three new taxa were independent species; 4) principal component analysis (PCA) and discriminant analysis showed clear separation in scatterplots from morphologically similar species; and 5) these three new taxa had distinct glans penis morphologies. Accordingly, three new taxa were described as *N. minor* **sp. nov.**, *N. kulakangria* **sp. nov.**, and *N. konggordous* **sp. nov.**

Key Words

Molecular phylogenetics, morphology, *Neodon*, new species, taxonomy

Introduction

The genus *Neodon* Horsfield, 1849, belongs to the family Cricetidae, order Rodentia. Traditionally, the only morphological diagnostic feature of this genus was the presence of three closed triangles in front of the posterior transverse space of the first lower molar. Hinton (1923, 1926) included five species in this genus: *Neodon sikimensis*, *N. irene*, *N. forresti*, *N. oniscus*, and *N. carruthersi*. Allen (1940) recognized three species: *N. sikimensis*, *N. irene*, and *N. forresti*. Ellerman (1941) later added *N. juldanschi* to this genus based on Hinton's arrangement (1923, 1926). Ellerman and Morrison-Scott (1951) listed four species: *N. sikimensis*, *N. irene*, *N. carruthersi*, and *N. juldanschi*, while Wilson and Reeder (1993) placed *N. sikimensis*, *N. irene*, and *N. juldanschi* in subgenus *Neodon* (genus *Microtus*). Similarly, Wilson and Reeder (2005) recognized *N. sikimensis*, *N. irene*, *N. forresti*, and *N. juldanschi*.

The application of molecular biology has provided an effective approach for phylogenetic studies. By integrating molecular biology and morphological research, Liu et al. (2012, 2017, 2022) and Pradhan et al. (2019)

revealed that the biodiversity of *Neodon* had been significantly underestimated. Liu et al. (2012) confirmed that *Lasiopodomys fuscus* and *Phaiomys leucurus* belonged to *Neodon* and identified *N. linzhiensis*, challenging the traditional diagnostic criterion of three closed triangles in front of the posterior transverse space of the first lower molar. Liu et al. (2017) reclassified *Microtus clarkei* as *N. clarkei* and described the new species *N. medogensis* and *N. nyalamensis*. Pradhan et al. (2019) described *N. nepalensis* based on molecular and morphological data. Liu et al. (2022) further expanded our understanding of diversity in *Neodon*, describing six new species (*N. bershulaensis*, *N. bomiensis*, *N. chayuensis*, *N. liaoruii*, *N. namchabarwaensis*, and *N. shergylaensis*) using morphological and whole-genome sequence data. Some of these new species and reclassified taxa possess four or five closed triangles in front of the posterior transverse space of the first lower molar. Currently, *Neodon* includes 16 recognized species.

Neodon occurs only in the Tibetan-Himalayan region (THR), which is recognized as one of the world's hotspots for genetic diversity. Recent publications on newly described small mammal species (e.g., Ge et al. 2021; Liu et al. 2022; Chen et al. 2021; Chen et al. 2024) demonstrated that surveying unexplored areas in this region is likely to result in the discovery of new species. Therefore, additional surveys in unexplored regions are likely to lead to the discovery of new species.

During recent surveys of the small mammal fauna in Sichuan and southern Xizang, China, we collected several specimens of *Neodon* that differ from other congeneric species in morphological and molecular characteristics. Morphological and molecular analyses of *Neodon* necessitates the descriptions of three new species.

Materials and methods

Ethics statement

All specimens were obtained in accordance with the guidelines of the American Society of Mammalogists and the laws and regulations of China concerning the protection of wild terrestrial animals (State Council Decree 1992; Sikes and Animal 2016). Field collection protocols were approved by the Ethics Committee of the Sichuan Academy of Forestry (under project number 2023-001). Voucher specimens were deposited at the Sichuan Academy of Forestry (Chengdu, China).

Samples and sequencing

A total of 63 tissue samples were used in the molecular analysis, including 15 described *Neodon* species (*N. bershulaensis*, *N. bomiensis*, *N. chayuensis*, *N. clarkei*, *N. forresti*, *N. fuscus*, *N. irene*, *N. leucurus*, *N. liaoruii*, *N. linzhiensis*, *N. medogensis*, *N. namchabarwaensis*, *N. nyalamensis*, *N. shergylaensis*, and *N. sikimensis*) and three unknown species (Fig. 1, Suppl. material 1: table S1). *Alexandromys maximowiczii*, *A. limnophilus*, *A. fortis*, *Lasiopodomys brandtii*, *L. gregalis*, *Myodes rutilus*, *M. rufocanus*, *Eothenomys eva*, *E. cachinus*, *E. melanogaster*, *Microtus agrestis*, and *M. ilaeus* were used as outgroups.

Total DNA was extracted using the Animal Tissue Genomic DNA Rapid Extraction Kit (Chengdu Fuji Biotechnology Co., Ltd., Sichuan, China). Two mitochondrial genes (cytochrome b [*CYTB*, 1,143 bp] and NADH dehydrogenase subunit 2 [*ND2*, 917 bp]) and three nuclear genes (interphotoreceptor retinoid-binding protein [*IRBP*, 1,235 bp], recombination activating 1 [*RAG1*, 1,021 bp], and growth hormone receptor [*GHR*, 843 bp]) were sequenced for phylogenetic analysis. Primer pairs were obtained from the literature (Teeling et al. 2000; Galewski et al. 2006; He et al. 2010; Cheng et al. 2017) (Suppl. material 1: table S2). The PCR cycling parameters were 94 °C for 5 min; 40 cycles of 45 s at 94 °C, 45 s at 49–56 °C, and 90 s at 72 °C; and a final extension of 10 min at 72 °C. These genes were selected as they have served as effective genetic markers for assessing phylogenetic relationships among certain mammals (He et al. 2017; Meredith et al. 2011). The PCR products were sequenced at the Sangon Sequencing Center (Chengdu, China). All generated DNA sequences were deposited in GenBank with their corresponding accession numbers (Suppl. material 1: table S1). In addition, some available *CYTB* and *ND2* sequences of *Neodon* were downloaded from GenBank for downstream analysis (Suppl. material 1: table S1), including *N. nepalensis* (Liu et al. 2017, 2022; Zhao et al. 2017; Wu et al. 2022).

Phylogenetic analyses and species delimitation

Phylogenetic analyses were conducted using the following three datasets: mitochondrial genes (mtDNA), all genes (mt+nuDNA), and nuclear genes (nuDNA). Two approaches were used for the phylogenetic reconstruction. First, the JMODELTEST v2.1.7 (Darriba et al. 2012) was used to identify the optimal model for each gene. The fitness of the model was evaluated using the Akaike information criterion (Luo et al. 2010), and the best models for each gene have been shown in Supporting Information (Suppl. material 1: table S2). MrBayes v3.1.2 (Ronquist and Huelsenbeck 2003) was used for the Bayesian inference analysis. Each run was performed using four Markov chain Monte Carlo (MCMC) algorithms, with 10,000,000 generations for a single-gene dataset and 30,000,000 generations for concatenated gene datasets. All runs were sampled every 10,000 generations. Convergence of the runs was accepted when the average standard deviation of the split frequencies was < 0.01. Tree nodes were considered strongly supported when ultrafast bootstrap values (BSP) were ≥ 95 and posterior probabilities (pp)

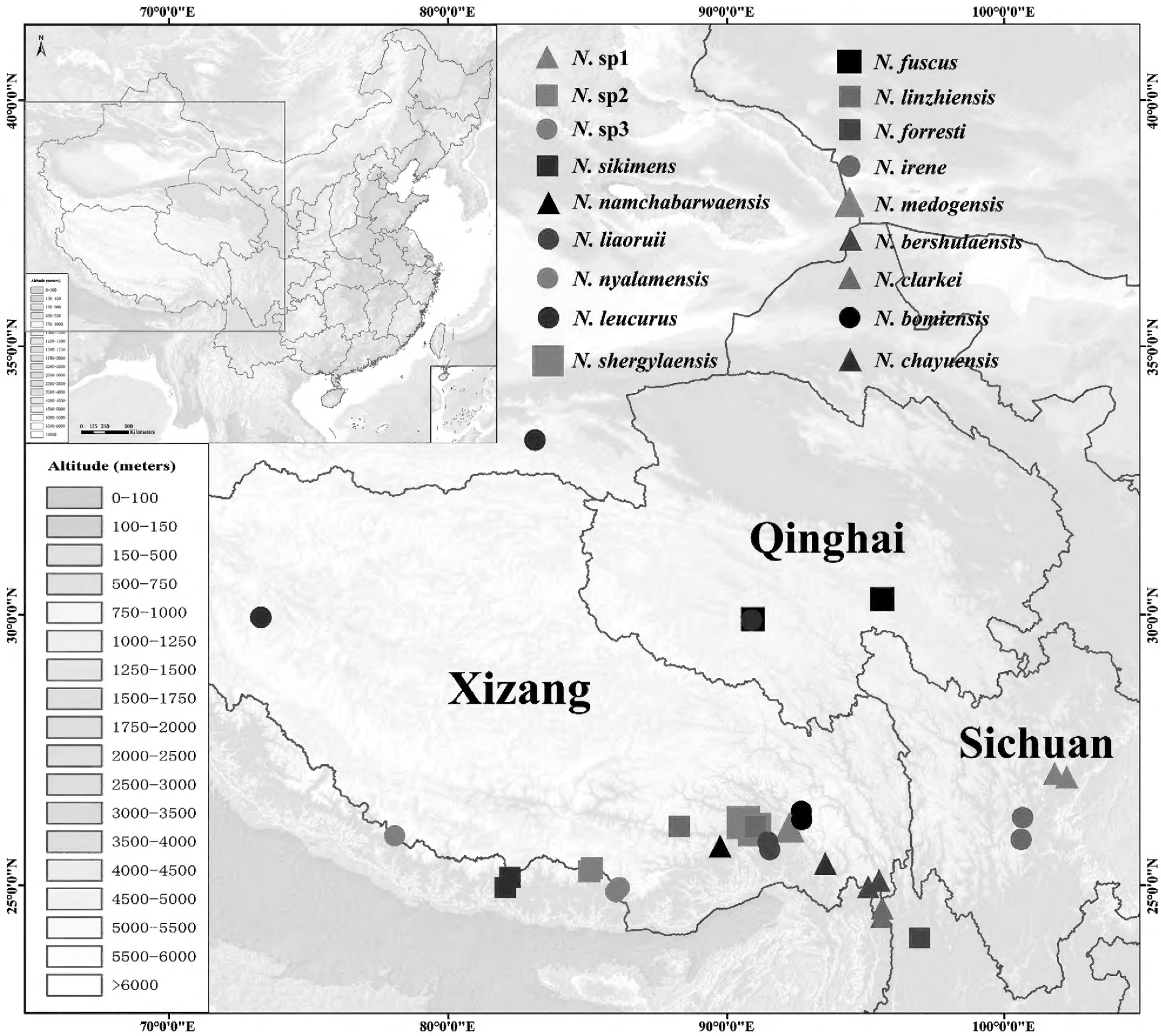

Figure 1. Specimen collecting sites of *Neodon* in China in this study.

were ≥ 0.95 (Heled and Drummond 2010). Second, RAXML v7.2.8 (Stamatakis et al. 2008) was used for maximum likelihood (ML) analyses on the CIPRES Science Gateway v3.1 (Miller et al. 2010) (http://www.phylo.org). We used the GTR+GAMMA model for each partition, as recommended by RAXML, selected the rapid bootstrapping algorithm (Stamatakis et al. 2008), and ran 500 bootstrap replicates. Nodes of the ML trees with BSP ≥ 70 were considered well supported.

Genetic distances were calculated based on *CYTB* using the Kimura 2-Parameter (K2P) model (Kimura, 1980) in MEGA v11.0 (Tamura et al. 2021) with 1,000 bootstrap replications. Two empirical methods were used to test the species boundaries. Automatic barcode gap discovery (ABGD) (Puillandre et al. 2012), a distance-based barcode approach, was used to define the barcode gap for *CYTB*. The estimated transition/transversion bias was computed using MEGA v11.0 (Tamura et al. 2021). The ABGD analysis was performed using https://bioinfo.mnhn.fr/abi/public/abgd (Puillandre et al. 2012). First, the K80 distance and X values (0.25, 0.5, 0.75, and 1.0) were selected. The remaining parameters were set to default values (Pmin = 0.001, Pmax = 0.1, steps = 10, and number of bins = 20). Second, BPP v4.7.0 (Yang and Rannala 2010) was used to test the independent evolutionary lineage hypothesis of these populations under multi-species fusion (Yang and Rannala 2010). Datasets 2 (mtDNA + nuDNA) and 3 (nuDNA) were used in the analysis. Both 'A10' (Yang and Rannala 2010; Rannala and Yang 2013) and 'A11' (Yang and Rannala 2014) analyses with different θ (ancestral population sizes) and τ0 (divergence time among species) priors were performed for each dataset. BPP 'A10' analysis was performed for species delimitation of a given species tree, while the 'A11' analysis was performed for both species tree estimation and species delimitation; the previously constructed gene tree was used as a guide tree in the 'A10' analysis. We sampled every 50 generations for 100,000 samples for each run, and the first 20,000 samples were discarded as burn-in. Analyses were conducted in duplicate to ensure consistency. Each clade was considered an independent species if the posterior probability was > 0.95.

Morphological analyses

In total, 109 preserved specimens of *Neodon*, including *N. sikimensis*, *N. shergylaensis*, *N. nyalamensis*, *N. namchabarwaensis*, *N. medogensis*, *N. linzhiensis*, *N. liaoruii*, *N. leucurus*, *N. fuscus*, *N. forresti*, *N. chayuensis*, *N. bomiensis*, *N. bershulaensis*, *N. irene*, *N. clarkei*, and the three unknown specimens, were morphologically examined. The following external measurements were obtained in the field: head–body length (HBL), tail length (TL), hindfoot length (HL), and ear length (EL). Skull measurements followed those of Liu et al. (2012, 2017, 2022). A digital display Vernier caliper (accurate to 0.01 mm) was used to measure 10 indices: greatest length of the skull (GLS), skull basal length (SGL), condylobasal length (CBL), zygomatic breadth (ZB), mastoidal breadth (MB), braincase height (BH), width across molars (M-M), upper molar row length (UML), lower molar row length (LML), and mandibular length (ML). Measured specimens were listed in the Supporting Information (Suppl. material 1: table S3). The overall similarity between species was evaluated using principal component analysis (PCA), provided that all data were normally distributed. A discriminant analysis was performed to determine whether the classification of the specimens was accurate. All measured data were analyzed using SPSS software v26.0 (SPSS, Chicago, IL, USA).

The morphological characteristics of the male genitalia were recorded. Variation in male external genitalia has long been used as an important taxonomic characteristic in mammals (Hooper and Musser 1964; Lidicker 1968; Sullivan et al. 1990), playing a potential role in reproductive isolation among species (Patterson and Thaeler 1982; Matocq et al. 2007). Glans penises of adult male specimens were prepared following the methods of Hooper (1958) and Lidicker (1968). Briefly, the fresh glans collected from the field were immediately preserved in 75% ethanol until further processing. Samples were subsequently placed in a 4% solution of KOH until the soft tissues became transparent and the baculum was faintly visible. Staining was done in a 0.003% solution of Alizarin Red until the bones became purplish red. This was followed by placing the specimens successively in 25%, 50%, and 75% glycerol and finally storing them in 100% glycerol. The dissection was performed under the anatomical lens, and the morphologies of the urethral lappet, dorsal papilla, and outer crater papilla were observed, described, and drawn as figures.

Results

Phylogenetic relationships and species delimitation

The trees from Bayesian and ML analyses for each dataset produced similar topologies. Therefore, only the Bayesian phylogenetic trees are presented here (Fig. 2A, C, D). Trees based on the three datasets consistently divided *Neodon* into 19 clades, containing three unnamed clades, denoted as *N.* sp1, *N.* sp2, and *N.* sp3, in addition to the 16 described species. However, the topologies of the three trees exhibited inconsistencies. In both the mt+nuDNA and mtDNA trees, *N.* sp1, *N. linzhiensis*, *N. fuscus*, and *N. irene* formed a larger clade, whereas in the nuDNA tree, *N.* sp1 appeared as a monophyletic lineage. The mt+nuDNA tree showed that *N.* sp2 and *N. nepalensis* were sister species and shared a common ancestor with *N. sikimensis*. In contrast, the mtDNA tree suggested that *N.* sp2 and *N. sikimensis* were sister species, while *N. nepalensis* occupied the most basal position among all *Neodon* species. The nuDNA tree topology indicated that *N.* sp2 shared a common ancestor with the sister species *N. nyalamensis* and *N.* sp3. In both the mt+nuDNA and mtDNA trees, *N.* sp3 consistently formed a sister relationship with *N. leucurus*. The posterior probability of each clade was > 0.95, and the bootstrap support was > 85. However, the posterior probability and bootstrap support were lower for several nodes on the trunk of the tree (posterior probability < 0.95, bootstrap support < 50), and the relationship between these species remains unclear (Huelsenbeck and Hillis 1993; Leaché and Reeder 2002).

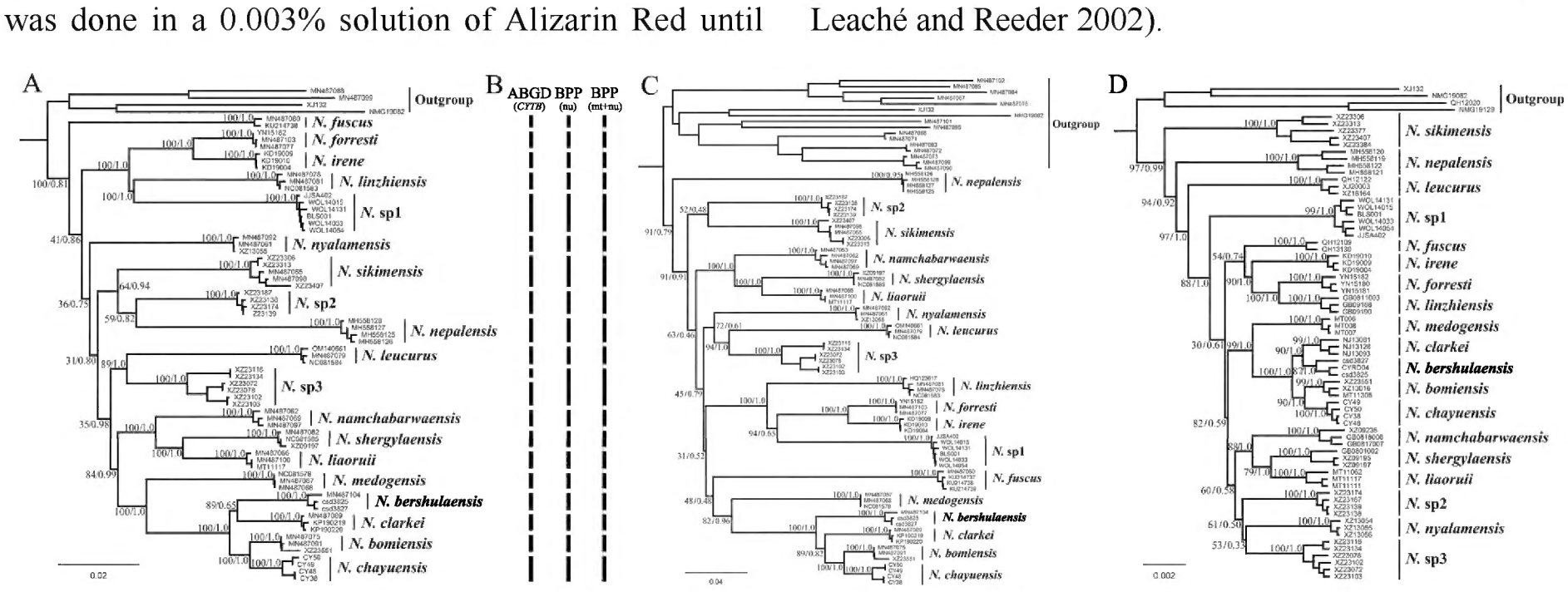

Figure 2. Bayesian phylogenetic trees based on three datasets (**A.** mtDNA+nuDNA; **C.** mtDNA; **D.** nuDNA) (left: ultrafast bootstrap values; right: BI posterior probabilities) and species delimitation results (**B**).

The K2P genetic distances of *CYTB* gene among the 16 described and three unknown species of *Neodon* showed that the genetic distance ranged from 4.0% to 15.5% (average: 12.0%, Table 1), with the lowest and highest values observed between *N. bomiensis* and *N. chayuensis* and *N.* sp1 and *N. bershulaensis*, respectively. The genetic distance between *N.* sp1 and the other 18 species ranged from 10.7% (*N. forresti*) to 15.5% (*N. bershulaensis*), with an average distance of 13.3%. The genetic distance between *N.* sp2 and the other 18 species ranged from 9.9% (*N. liaoruii*) to 13.3% (*N. fuscus*), with an average distance of 11.6%. The genetic distance between *N.* sp3 and the other 18 species ranged from 9.0% (*N. liaoruii*) to 13.0% (*N. linzhiensis*), with an average distance of 10.9%. Genetic distances between all species exceeded 10%, a value usually found in geographically dispersed species of different organisms (Baker and Bradley 2006).

The BPP results for both datasets supported 19 species (Fig. 2B). The ABGD analysis based on different X values (0.25, 0.5, 0.75, and 1.0) identified 20 species, with *N. sikimensis*, *N. shergylaensis*, *N. nyalamensis*, *N. namchabarwaensis*, *N. medogensis*, *N. linzhiensis*, *N. liaoruii*, *N. leucurus*, *N. fuscus*, *N. forresti*, *N. chayuensis*, *N. bomiensis*, *N. bershulaensis*, *N.* sp1, *N. irene*, *N. clarkei*, *N.* sp2, and *N. nepalensis* as separate species, and *N.* sp3 identified as two species (Fig. 2B).

Morphological results

The dental characteristics and appearance of the known and novel species of *Neodon* were summarized in Table 2. Based on the two most stable molar features—the number of closed triangles before the posterior transverse space of the first lower molar and the number of inner angles of the second upper molar—14 of these putative species formed three groups in the PCA and discriminant analysis. The first group contained *N. forresti*, *N. irene*, *N. leucurus*, *N. liaoruii*, *N.* sp1, and *N. sikimensis*, all of which have three closed triangles in front of the posterior transverse space of the lower first molar and two inner angles of the upper second molar. The Kaiser–Meyer–Olkin (KMO) value was 0.907, and Bartlett's test was significant ($p = 0.000$), indicating that the data were suitable for PCA. The first two PCs were selected for the analysis of the first group and explained 95.45% of the variance. All measurements had positive scores on PC1, which explained 89.33% of the total variation, suggesting a relationship with the overall specimen size. PC2, explaining 6.18% of the total variation, was dominated by UML and LML. The PCA separated *N.* sp1 from all the other species. The discriminant analysis results showed that 100% of the specimens were accurately classified based on cranial measurements, and *N.* sp1 could be distinguished from the other species (Fig. 3A, B).

All species in the second group (*N.* sp3, *N. liaoruii*, *N. namchabarwaensis*, *N. nyalamensis*, and *N. shergylaensis*) had three closed triangles in front of the posterior transverse space of the lower first molar and three inner angles in the upper second molar. The KMO value was 0.757, and Bartlett's test was significant ($p = 0.000$). The explanatory degree of PC1 was the highest, at 53.15%, with all factor loadings being positive. Factor loadings of ML, GLS, SGL, and ZB were > 0.8. The explanatory degree of PC2 was 18.63%, dominated by LML, UML, and BH. The discriminant analysis results, but not the PCA, distinguish these species, including distinguishing *N.* sp3 from the other four species (Fig. 3C, D). The discriminant analysis results showed that 93.5% of the specimens were accurately classified. One specimen of *N. shergylaensis* was misidentified as *N. namchabarwaensis*, and one specimen of *N. namchabarwaensis* was misidentified as *N. shergylaensis*.

The third group included *N. bershulaensis*, *N. clarkei*, *N.* sp2, and *N. linzhiensis*, all of which had five closed triangles in front of the posterior transverse space of the first lower molar. The KMO value was 0.850, and Bartlett's test was significant ($p = 0.000$).

Table 1. K2P distance between species of *Neodon* based on the *CYT B* gene in this study.

Species	*N.* sp1	*N. ber*	*N. cha*	*N. lin*	*N. ire*	*N. clar*	*N. fus*	*N. nep*	*N. nya*	*N. nam*	*N. sik*	*N. lia*	*N. med*	*N. bom*	*N. for*	*N. leu*	*N. she*	*N.* sp3	*N.* sp2
N. sp1																			
N. bershulaensis	0.155																		
N. chayuensis	0.144	0.074																	
N. linzhiensis	0.130	0.148	0.139																
N. irene	0.109	0.125	0.121	0.120															
N. clarkei	0.150	0.074	0.065	0.137	0.127														
N. fuscus	0.148	0.141	0.145	0.145	0.129	0.135													
N. nepalensis	0.133	0.152	0.148	0.154	0.136	0.154	0.155												
N. nyalamensis	0.123	0.125	0.118	0.129	0.109	0.121	0.131	0.143											
N. namchabarwaensis	0.144	0.118	0.110	0.119	0.105	0.113	0.145	0.138	0.109										
N. sikimensis	0.130	0.127	0.106	0.118	0.109	0.116	0.127	0.128	0.101	0.109									
N. liaoruii	0.130	0.114	0.111	0.133	0.117	0.111	0.128	0.129	0.105	0.082	0.110								
N. medogensis	0.126	0.128	0.117	0.128	0.120	0.115	0.145	0.133	0.128	0.107	0.127	0.101							
N. bomiensis	0.139	0.070	0.040	0.136	0.110	0.063	0.126	0.142	0.110	0.104	0.106	0.108	0.108						
N. forresti	0.107	0.133	0.133	0.115	0.051	0.140	0.133	0.133	0.115	0.112	0.117	0.119	0.119	0.126					
N. leucurus	0.149	0.133	0.130	0.142	0.115	0.128	0.135	0.143	0.126	0.121	0.114	0.115	0.138	0.126	0.117				
N. shergylaensis	0.126	0.141	0.125	0.131	0.128	0.133	0.146	0.127	0.114	0.094	0.127	0.072	0.117	0.122	0.122	0.126			
N. sp3	0.128	0.111	0.100	0.130	0.117	0.101	0.123	0.123	0.095	0.100	0.102	0.090	0.119	0.094	0.124	0.103	0.095	0.109	
N. sp2	0.124	0.129	0.123	0.131	0.105	0.126	0.133	0.123	0.117	0.105	0.107	0.099	0.117	0.115	0.105	0.119	0.112	0.101	0.116

Table 2. The dental characteristics and appearance of the species of *Neodon*.

Species	The number of closed triangles before the posterior transverse space of the first lower molar	The number of inner angles of the second upper molar	The number of inner angles of the third upper molar	The number of outer angles of the third upper molar	Tail length / Head-body length
N. fuscus	4	2	3	3	29%
N. linzhiensis	5	2	50%4; 50%3	3	30%
N. forresti	3	2	3	3	30%
N. irene	3	2	20%4, 80%3	3	37%
N. sp1	3	2	4	3	38%
N. leucurus	3	2	3	3	30%
N. namchabarwaensis	3	3	4	3	40%
N. sikimensis	3	2	50%4, 50%3	3	45%
N. nepalensis	3	2	40%4; 60%3	3	24%
N. nyalamensis	3	3	4	80%4; 20%3	41%
N. shergylaensis	3	3	4	3	37%
N. liaoruii	3	34%2; 66%3	60%4; 40%3	3	51%
N. sp2	5	3	4	3	48%
N. sp3	3	3	4	3	40%
N. medogensis	4	3	4	80%4; 20%3	48%
N. bershulaensis	5	3	4	3	48%
N. clarkei	5	3	4	3	55%
N. bomiensis	4	3	3	3	48%
N. chayuensis	4	3	3	3	45%

The explanatory degree of PC1 was the highest, at 53.15%, and all factor loadings were > 0.8. The explanatory degree of PC2 was 18.63%, and it was dominated by LML and M-M. The scatterplots showed that all four species exhibited separation between described species (Fig. 3E, F). The results of the discriminant analysis showed that 100% of the specimens were accurately classified based on cranial measurements, and all species exhibited a good separation trend.

In comparison of glans penis morphology (Fig. 3), the three new taxa exhibited distinct proximal, distal, and lateral bacula, urethral lappet, and dorsal papillae. The quantity of crater papillae also differed from those of similar species in terms of molecular characteristics and morphology. For example, *N.* sp3 was closely related to *N. leucurus* in the molecular phylogeny; however, morphologically, it was more similar to *N. nyalamensis*. The glans penis of *N.* sp3 had 3–4 outer crater papillae, while *N. leucurus* had 7–8. Additionally, *N.* sp3 had dorsal papillae with two forks, compared to one fork in *N. leucurus*. Its urethral lappet had three forks, compared to two in *N. leucurus*. The base of the proximal baculum was trapezoid-shaped in *N.* sp3, while it was ellipse-shaped in *N. leucurus*, and *N.* sp3 had long lateral bacula, whereas *N. leucurus* had very short bacula. Furthermore, the glans penis of *N.* sp3 differed significantly from that of *N. nyalamensis* in terms of the proximal, distal, and lateral baculum as well as the urethral lappet.

Taxonomic account

Neodon minor Wang & Liu, sp. nov.

https://zoobank.org/4D665C7D-5BEC-4131-9493-5DF3DA5F79CF

Note. Unnamed clade *N.* sp1

Holotype. An adult female, field number JJSA384 (Museum number SAF09244), collected from Baoxing County, Sichuan, by Rui Liao on 2 September 2009. The specimen was prepared as skin with a cleaned skull and deposited at the Sichuan Academy of Forestry.

Type locality. Jiajin Mountains, Baoxing County, Sichuan, China; 30.83635°N, 102.70953°E; 3,460 m a.s.l.

Measurements of holotype. Weight, 28 g; HBL, 92 mm; TL, 37 mm; HFL, 15 mm; EL, 13 mm; SGL, 23.62 mm; SBL, 22.31 mm; CBL, 23.26 mm; ZB, 13.31 mm; IOW, 3.22 mm; MB, 11.17 mm; SH, 8.51 mm; ABL, 6.54 mm; LMxT, 5.31 mm; LMbT, 5.28 mm; M-M, 4.52 mm; ML, 13.72 mm; and LEPILM, 7.94 mm.

Paratypes. Twelve specimens (7 ♂♂, 5 ♀♀), skins with skulls, and male specimens with glans penis. Seven specimens (JJSA382 [SAF09242], ♂; JJSA383 [SAF09243], ♀; JJSA385 [SAF09245], ♂; JJSA386 [SAF09246], ♂; JJSA487 [SAF09347], ♂; JJSA491 [SAF09350], ♀; and JJSB010 [SAF09374], ♀) from Jiajin Mountains. One specimen (BLS001 [SAF09779], ♂) from the Balang Mountains. Four specimens (WOL14015 [SAF14245], ♂; WOL14033 [SAF14263], ♀; WOL14103 [SAF14333], ♂; and WOL14131 [SAF14361], ♀) from the Wolong National Nature Reserve. All specimens were collected by Rui Liao.

Geographic distribution. This new species has been recorded in most areas of the Qionglai Mountains, Sichuan, China, including the Jiajin and Balang Mountains, Wolong National Nature Reserve, and Xiling Snow Mountain.

Etymology. The species epithet was derived from its being the smallest species of *Neodon*. Common names: Lesser Mountain Vole, 小松田鼠 (Xiao Songtianshu).

Diagnosis. The smallest species of *Neodon*, where adult HBL does not exceed 100 mm and TL comprises nearly 38% of the HBL. Upper incisors straight, not tilting forward. Lower first molars with three closed triangles in front of posterior transverse space, five inner angles, and three outer angles. Second upper molar without posterior inner angle, with two inner and three outer angles. Third upper molar with four inner and three outer angles. Distribution of *N. minor* sp. nov.

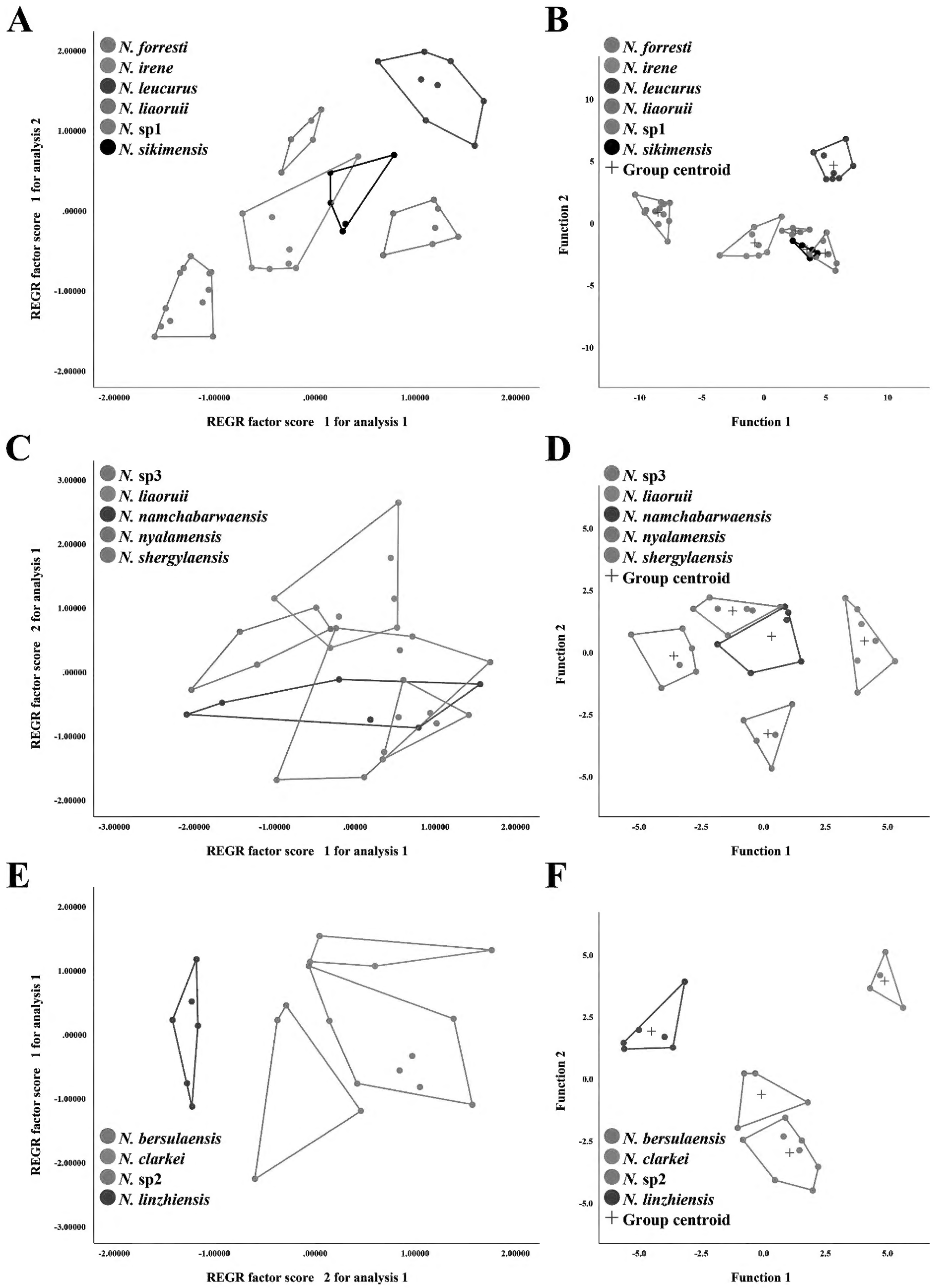

Figure 3. Principal component analysis results based on skull measurement data of genus *Neodon* (**A.** First group; **C.** Second group; **E.** Third group) and canonical discriminant analysis results (**B.** First group; **D.** Second group; **F.** Third group).

near to that of *N. irene*, but allopatric, occurring at a higher elevation. Tooth patterns similar. Skull of *N. irene* much larger than that of *N. minor* sp. nov., and the third upper molar of *N. irene* typically with three inner and three outer angles, while that of *N. minor* sp. nov. with four inner and three outer angles.

Description. General pelage color of holotype brown, with back fur approximately 10 mm long. Proximal part

of fur black-gray, while the distal parts brown, with an indistinct color boundary between the dorsal and ventral fur. Ventral fur gray-white with a black-gray base, uniform color from throat to belly and anus. Pelage of paratypes same as that of the holotype. Mystacial vibrissae mostly brown, but some black, with approximately 20 on each side. Shortest vibrissa approximately 4 mm, and longest approximately 27 mm. Ears projected slightly above pelage. A rim present on the front and entire back, with dense brown fur. Color on the top and underside of tail consistently tan, similar to dorsal fur. Hairs on the tip of tail slightly longer. Forelimb hairs were gray-white, hindlimb pelage gray-brown (Fig. 4C1–C3). Claws yellow-white, with long, stiff hair. Five palmar pads and six plantar pads. Females with two pectoral and two inguinal pairs of mammae. Skull sturdy (Fig. 5C) and straight in dorsal profile, nasal bridge slightly arched, and braincase approximately orbicular. Nasal bones broad anteriorly and narrow posteriorly. Posterior and anterior frontal bones broad but narrow in the middle. Interparietal bone broad, trapezoid-shaped. Distinct ridges in interorbital space, elderly individuals having two ridges forming a crest. Two ridges behind temporal joint above auditory bulla. Zygomatic arches sturdy. Auditory bullae medium-sized. Posterior palate typical of Arvicolinae, continuing as a narrow bridge and separating two lateral pits. Palatine and pterygoid with many small foramina. Mandibles sturdy. Upper incisors straight with lip-sides light orange. First upper molar with four closed triangles after anterior transverse space (two inner and two outer), forming three inner and three outer angles. Second upper molar with three closed triangles after the anterior transverse space (one inner and two outer), forming two inner and three outer angles. Third upper molar transverse prism-like, followed by two small outer triangles, one larger inner closed triangle, and a C-shaped loop, forming four inner and three outer angles. Lower incisors relatively long, and lip sides light orange. First lower molar with three closed triangles anterior to posterior transverse space; anterior space large and anomalistic, forming two inner and two outer angles, with five inner and four outer angles. Second lower molar with three inner and three outer angles. Third lower molar with three transverse lobes, forming three inner and three outer angles. Glans penis smaller than that of other *Neodon* species (Fig. 6C). Exterior of gland stick-shaped with a ventral groove. Outer crater papillae absent. Most specimens with urethral lappets forked into three branches, middle branch slightly lower; a few specimens with only two branches. Two shapes of dorsal papillae: most specimens with two cusps, a few with only one cusp. Proximal, distal, and lateral bacula bony. Proximal baculum slightly enlarged and spoon-shaped. Distal baculum thick and stick-shaped. Lateral baculum stick-shaped and short.

Habitat. This species inhabited alpine shrubs and alpine meadows at elevations ranging from 3,400 to 4,300 m. It typically digs holes approximately 20 mm in diameter, usually in grass or under shrub roots.

Neodon kulakangria Wang & Liu, sp. nov.

https://zoobank.org/2DB7431C-2477-47F2-AF92-C3BB44337352

Note. Unnamed clade *N.* sp2

Holotype. An adult female, field number XZ23162 (Museum number SAF230542), collected from Luozha (Lhozhag) County, Xizang (Tibet), by Xuming Wang on August 23, 2023. Specimen preserved as a skin with a cleaned skull and deposited at the Sichuan Academy of Forestry.

Type locality. East of Kulagangri (Kula Kangri) Mountains, Lajiao Village, Luozha County, Xizang, China; 28.081162°N, 91.029954°E; 3,200 m a.s.l.

Measurements of holotype. Weight, 45 g; HBL, 120 mm; TL, 60 mm; HFL, 22 mm; EL, 16 mm; SGL, 28.82 mm; SBL, 26.83 mm; CBL, 28.76 mm; ZB, 15.63 mm; IOW, 4.11 mm; MB, 13.01 mm; SH, 9.94 mm; ABL, 8.11 mm; LMxT, 6.75 mm; LMbT, 6.62 mm; M-M, 5.62 mm; ML, 19.65 mm; and LEPILM, 8.21 mm.

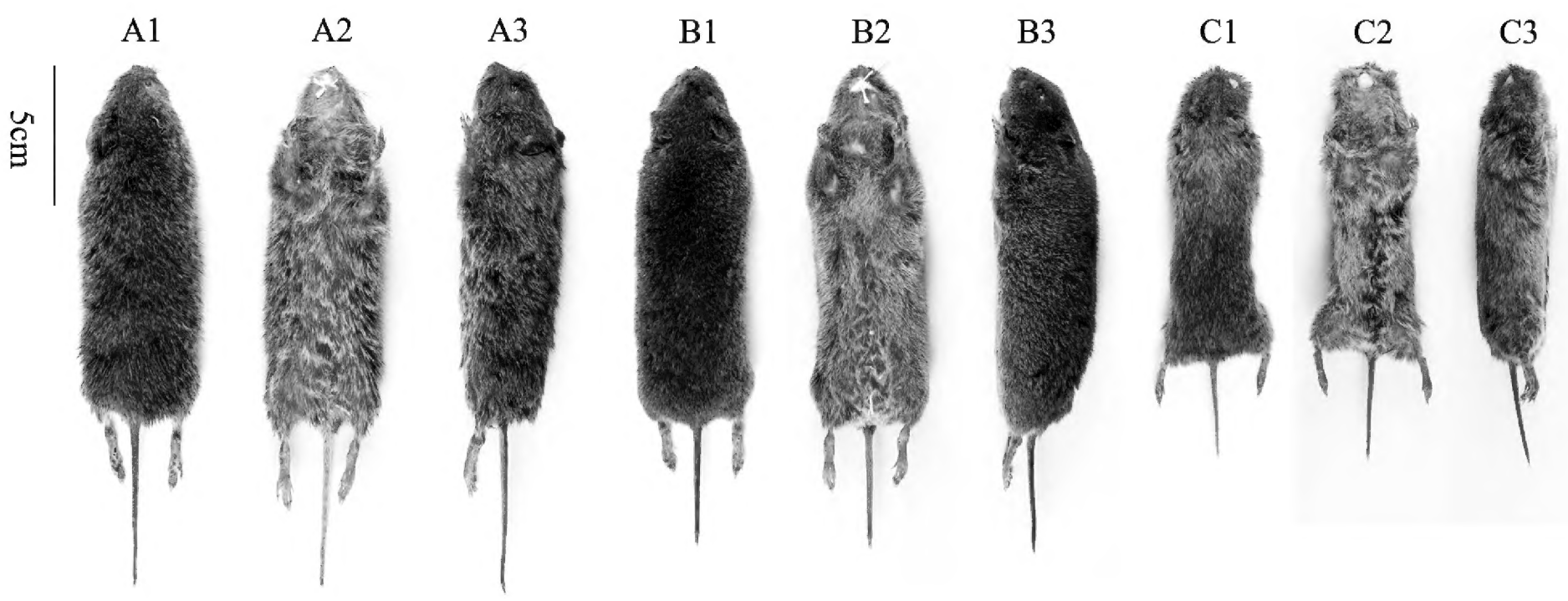

Figure 4. Dorsal, ventral, and lateral views of *N. kulakangria* sp. nov. (**A1–A3**), *N. konggordous* sp. nov. (**B1–B3**), and *N. minor* sp. nov. (**C1–C3**).

Figure 5. Dorsal, ventral, and lateral views of the skull and dorsal and lateral views of the mandible of *N. kulakangria* sp. nov. (**A**), *N. konggordous* sp. nov. (**B**), and *N. minor* sp. nov. (**C**).

Paratypes. Twelve specimens (6 ♂♂, 6 ♀♀), with skins with skulls, including male specimens with glans penis. Six specimens (XZ23138 [SAF230518], ♂; XZ23140 [SAF230520], ♀; XZ23141 [SAF230521], ♀; XZ23158 [SAF230538], ♂; XZ23159 [SAF230539], ♀; XZ23161 [SAF230541], ♂) are topotypes, and six (XZ23174 [SAF230554], ♂; XZ23176 [SAF230556], ♀; XZ23187 [SAF230567], ♂; XZ23189 [SAF230569], ♂; XZ23190 [SAF230570], ♀; and XZ23192 [SAF230572], ♀) were collected from 10 km northeast of the type locality. All specimens were collected by Xuming Wang, Rui Liao, and Buqing Peng.

Geographic distribution. Known only from two sites in Luozha County, west of the Kulagangri Mountains.

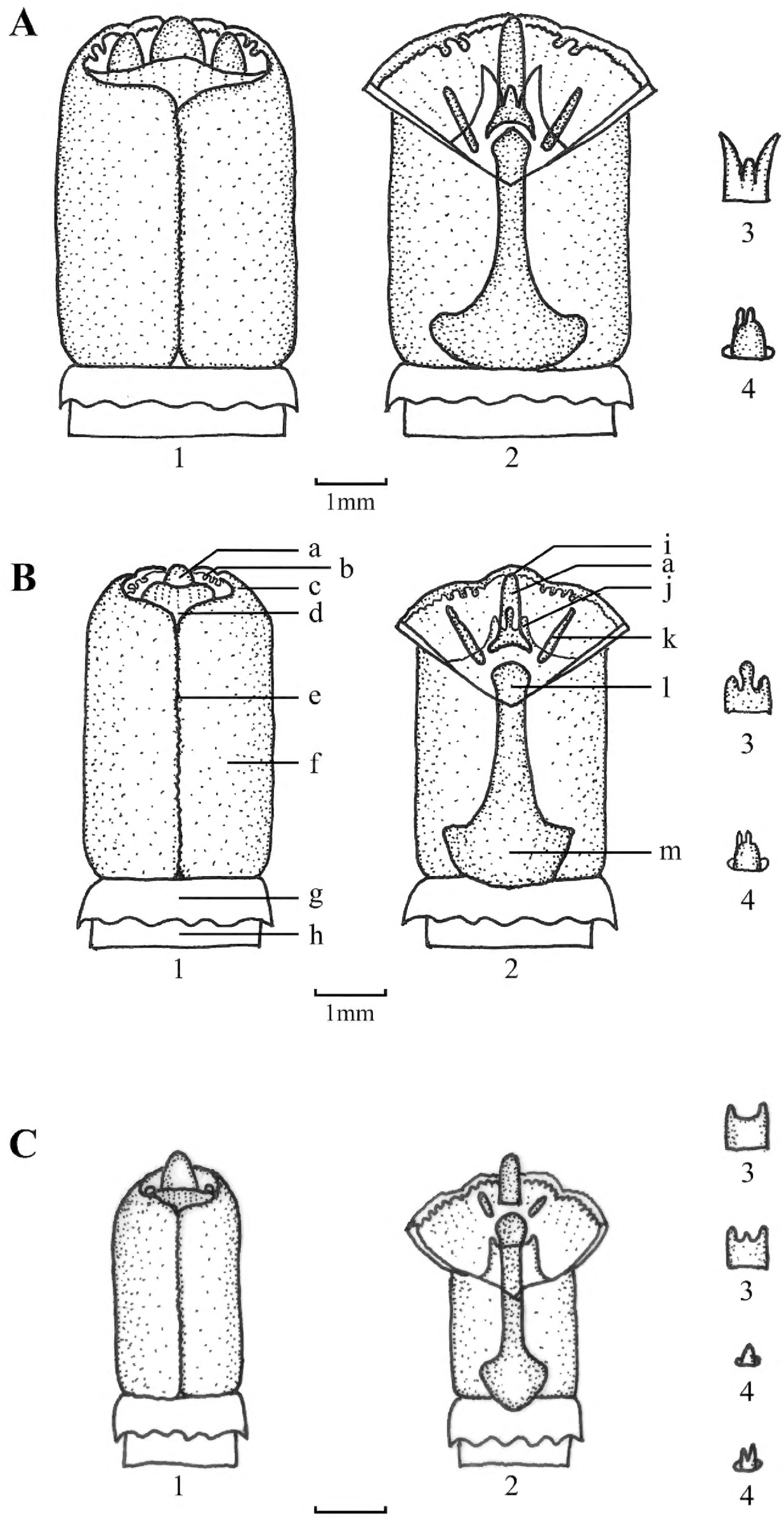

Figure 6. Penis of *N. kulakangria* sp. nov. (**A**), *N. konggordous* sp. nov. (**B**), and *N. minor* sp. nov. (**C**). Numbered structural features are as follows: 1. penis; 2. midventral cut view of glans; 3. urethral papilla; 4. dorsal papilla. Lowercase letter structural features are as follows: a. distal baculum; b. outer crater papillae; c. outer crater; d. urethral papilla; e. ventral groove; f. glans; g. prepuce; h. body of penis; i. tip of distal baculum; j. site of dorsal papilla; k. lateral baculum; l. proximal baculum; m. the base of proximal baculum.

Etymology. The name is derived from the Kulagangri Mountains. Common names: Kulagangri Mountain Vole, 库拉岗日松田鼠 (Kulagangri Songtianshu).

Diagnosis. An arvicoline with a typical palate of *Neodon*. First lower molar typically with five closed triangles, six inner angles, and five outer angles. First upper molar with

three closed triangles and a posterior inner angle, forming four inner and three outer angles. Second upper molar with a posterior inner angle, three inner angles, and three outer angles. Third upper molar with four inner and three outer angles. Larger individuals with HBL averaging over 117 mm, tail comparatively long, accounting for nearly 50% of the HBL. First lower molar with five closed triangles as in *N. linzhiensis*, *N. clarkei*, and *N. bershulaensis*. However, first upper molar of *N. kulakangria* sp. nov. with four inner and three outer angles, whereas *N. linzhiensis* and *N. clarkei* possess three inner and three outer angles, and *N. bershulaensis* with first upper molar having four inner and three outer angles in 70% of specimens, while the other 30% with three inner and three outer angles. *Neodon kulakangria* sp. nov. differs from *N. bershulaensis* by having a much larger second upper molar posterior inner angle. HBL of *N. kulakangria* sp. nov. greater than that of *N. bershulaensis*.

Description. General pelage color of the holotype gray-brown. Fur fine and approximately 10 mm long, with proximal part being black-gray and distal part brown. Color boundary between dorsal and ventral fur present but indistinct. Ventral fur gray-white with black-gray base, displaying a uniform color from throat to belly and anus. Pelages of paratypes consistent with those of the holotype. Mystacial vibrissae mostly white, with some having black proximal and white distal parts, approximately 20 on each side, shortest approximately 4 mm, and longest was approximately 27 mm. Ears protrude slightly above pelage, with a dense black-gray fur rim on front and entire backside. Dorsal tail black-gray, ventral part gray-white, lacking a clear color boundary. Hairs on tip of tail slightly longer. Both forelimb and hindlimb pelages black-gray. Claws yellow-white, with long, stiff hairs (Fig. 4A1–A3). Five palmar pads and six plantar pads. Females with two pectoral and one inguinal pair of mammae. Skull sturdy (Fig. 5A), with straight dorsal profile and braincase slightly oblate. Nasal bones anteriorly and narrow posteriorly. Posterior and anterior frontal broad at ends but narrow in middle. Interparietal broad and irregular. Faint ridges present in interorbital space; older specimens with two approaching ridges not usually forming a crest. Two ridges formed behind temporal joint above auditory bulla. Zygomatic arches sturdy, and auditory bullae large. Posterior palate typical of Arvicolinae, continuing as a narrow bridge and separating two lateral pits. Numerous foramina in palatines and pterygoids. Mandibles robust, and lip-sides of upper incisors orange. First upper molar with three closed triangles after anterior transverse space (two inner and one outer) and a posterior inner angle, forming four inner and three outer angles. Second upper molar with two closed triangles after anterior transverse space (one inner and one outer) and a posterior inner angle, forming three inner and three outer angles. Third upper molar with three closed triangles after the anterior transverse space (two inner and one outer) and a C-shaped loop, forming four inner and three outer angles. Lower incisors relatively long, and the lip-sides orange. First lower molar with five closed triangles in front of posterior transverse space, anterior space large and anomalistic, forming two inner and two outer angles, with six inner and five outer angles overall. Second lower molar with four closed triangles (two larger inner and two smaller outer) in front of posterior transverse space; front outer closed triangles created one inner and one outer angle, yielding four inner and three outer angles. Third lower molar with two closed triangles (one inner and one outer) in front of posterior transverse space; front closed triangles form one inner and one outer angle, resulting in three inner and three outer angles. Glans penis (Fig. 6A) sturdy, exterior stick-shaped with a ventral groove and two larger outer crater papillae on each side near dorsal flap. Urethral lappet having three branches, with very short middle branch. Conical dorsal papilla with two cusps arranged anteroposteriorly. Proximal, distal, and lateral bacula bony. Distal part of the proximal baculum enlarged and snake-head-shaped. Basal part of distal baculum enlarged, with a distal point and a terminal concave shape. Lateral baculum stick-shaped.

Habitat. This species inhabited mixed coniferous-broadleaved forests at elevations of 3,100–3,300 m, where trees reach approximately 15 m in height, and around 30% of the area was covered with dense herbaceous vegetation. This species was also observed in shrublands near farmlands.

Neodon konggordous Wang & Liu, sp. nov.

https://zoobank.org/CEE73EE0-9DAB-49BE-BD30-4014A3957CA8

Note. Unnamed clade *N.* sp3

Holotype. An adult female, field number XZ23131 (Museum number SAF230511), collected from Cuona (CoNa) County, Xizang (Tibet), by Xuming Wang on August 19, 2023. Specimen, prepared as a skin with a cleaned skull, was deposited at the Sichuan Academy of Forestry.

Type locality. West of Konggordo Mountains, Cuona County, Xizang, China; 27.923734°N, 91.838384°E; 3,870 m a.s.l.

Measurements of holotype. Weight, 43 g; HBL, 120 mm; TL, 43 mm; HFL, 21 mm; EL, 15 mm; SGL, 27.83 mm; SBL, 26.27 mm; CBL, 27.36 mm; ZB, 15.46 mm; IOW, 3.58 mm; MB, 12.88 mm; SH, 9.92 mm; ABL, 7.67 mm; LMxT, 6.56 mm; LMbT, 6.51 mm; M-M, 5.57 mm; ML, 19.94 mm; and LEPILM, 9.18 mm.

Paratypes. Ten specimens (8 ♂♂, 2 ♀♀), consisting of skins with skulls and male specimens with prepared glans penis. All specimens (XZ23072 [SAF230456], ♂; XZ23078 [SAF230462], ♂; XZ23080 [SAF230460], ♂; XZ23081 [SAF230465], ♂; XZ23103 [SAF230483], ♂; XZ23110 [SAF230490], ♂; XZ23130 [SAF230510], ♂; XZ23131 [SAF230511], ♀; XZ23133 [SAF230513], ♀; and XZ23134 [SAF230514], ♂) were collected from the type locality by Xuming Wang, Rui Liao, and Buqing Peng.

Geographic distribution. Known only from the western Konggordo Mountains, on both sides of the Dawang River (Tawang Chu) and Niangjiang Qu (Nyamjang Chu).

Etymology. The name is derived from the Konggordo Mountains. Common names: Konggordo Mountain Vole, 康格多松田鼠 (Kanggeduo Songtianshu).

Diagnosis. An arvicoline with the typical *Neodon* palate. Average adult HBL about 120 mm, with a TL of approximately 40% of the HBL. First lower molar with three closed triangles in front of posterior transverse space and six inner and five outer angles. Second upper molar lacking posterior inner angle, forming three inner and three outer angles. Third upper molar with four inner and three outer angles. *Neodon shergylaensis*, *N. nanchabarwaensis*, and *N. nyalamensis* similar to *N. konggordous* sp. nov. in TL-to-HBL ratio and tooth morphology. Compared to *N. shergylaensis*, with first lower molar having six inner and four outer angles, *N. nanchabarwaensis*, *N. nyalamensis*, and *N. konggordous* sp. nov. with a first lower molar with six inner and five outer angles. First upper molar of both *N. nanchabarwaensis* and *N. konggordous* sp. nov. with four inner and three outer angles, and 80% of individuals of *N. nyalamensis* with four inner and four outer angles. Body size of *N. nyalamensis* smaller than that of *N. nanchabarwaensis* and *N. konggordous* sp. nov. Anterior cap at front of first lower molar in *N. konggordous* sp. nov. usually forms a standard circular arc with smooth circular lines at the outer edge, but that of *N. nanchabarwaensis* with an irregular outer margin. Further, first pair of triangles behind the most anterior transverse prism of third upper molar of *N. nanchabarwaensis* connected, but *N. konggordous* sp. nov. with two unconnected closed triangles.

Description. General pelage color of the holotype black-brown, back darker, and sides lighter. Fur thick, about 14 mm long, proximal part black-gray, but distal part brown or black. Color boundary between the dorsal and ventral fur indistinct. Ventral side gray-white with black-gray base; coloration from the throat to belly and anus uniform. Pelage of paratypes the same as that of holotype. Mystacial vibrissae mostly white, but some with white proximal parts and black distal parts, approximately 25 on each side, shortest approximately 5 mm, and the longest was approximately 28 mm. Ears projected clearly above pelage, rim on front and entire backside covered with dense black-gray fur, edge with white fur. Dorsal part of the tail black-brown, ventral slightly lighter, without distinct color boundary. Pelage of forelimb and hindlimb gray-white. Claws yellow-white, with long, stiff hair (Fig. 4B1–B3). Five palmar and plantar pads. Females with two pectoral pairs and one inguinal pair of mammae. Skull sturdy (Fig. 5B), straight in dorsal profile. Nasal broad anteriorly, narrow posteriorly. Frontal broad at posterior and anterior ends, constricted in middle. Interparietal broad and nearly trapezoidal. Distinct ridges in interorbital space of adult specimens; two ridges form a crest. Two faint ridges behind the temporal joint, above the auditory bulla. Zygomatic arches robust, and auditory bullae relatively large. Posterior palate characteristic of Arvicolinae, continuing as a narrow bridge that separated both lateral pits. Numerous small foramina present in palatines and pterygoids. Mandibles sturdy. Upper incisors straight, projected downward, lip-side surfaces colored orange. First upper molar with three closed triangles posterior to anterior transverse space (two inner and one outer) and a posterior inner angle, forming four inner and three outer angles. Second upper molar with two closed triangles posterior to anterior transverse space (one inner and one outer) and a posterior inner angle, forming three inner and three outer angles. Third upper molar with three closed triangles posterior to anterior transverse space (one inner and two outer) and a C-shaped loop, forming four inner and three outer angles. Lower incisors relatively long, with orange lip-side surfaces. First lower molar with three closed triangles (two inner and one outer) in front of posterior transverse space, with two pairs of connected triangles in front. Anterior space semi-circular, typically forming a standard circular arc with a smooth outer edge. Molar with six inner and five outer angles. Second lower molar with three inner and three outer angles. Third lower molar with three irregular transverse lobes, forming three inner and three outer angles. Glans penis (Fig. 6B) robust, exterior stick-shaped, with ventral groove and 2–5 small outer crater papillae on each side of the lateral flap. Urethral lappet with three branches, middle branch very short with distal part enlarged. Conical dorsal papillae with two cusps arranged anterior-posteriorly. Proximal, distal, and lateral baculum bony; distal part of proximal baculum enlarged and pestle-shaped; basal part enlarged, tapering to a distal point, with a concave terminal end. Lateral baculum slender, with an enlarged basal part.

Habitat. This species inhabited alpine scrubs, subalpine coniferous forests, mixed coniferous broad-leaved forests, and secondary shrubs, artificial tea gardens, and other habitats, occupying a wide elevation spanning 2,810–4,350 m. Sympatric species include *Soriculus nigrescens*, *Niviventer eha*, *N. gladiusmaculus*, *Micromys erythrotis*, and *Ochotona macrotis*.

Discussion

Our molecular and morphological analyses reveal three new species of *Neodon*. This increases the number of species in the genus from 16 to 19, expanding our understanding of the diversity within *Neodon*. Tectonic activity of the Qinghai-Tibet Plateau blocked the ancient southwestern monsoon, leading to the formation of the southern branch of the westerly jet stream. This process is responsible for the plateau's environment changing from cold and dry to a more humid condition, providing a key habitat background for the diversification of *Neodon* (Liu et al. 2022). During the Pleistocene glacial period (which began approximately 2.6 million years ago), temperature decreases forced the ancestors of *Neodon* to migrate southward or eastward to the edges of the Qinghai-Tibet Plateau. The complex topography of these regions—including mountains, rivers, and "sky island" refugia—intensified geographic isolation, leading to speciation. *Neodon kulakangria* sp. nov. was discovered on the southern slopes of the Himalayas, within the region extending from the eastern side of the Kulakangri Mountains to the western side of the Dalariji Mountains. This species is a typical example of speciation influenced by geographic isolation due to "sky islands." Similarly, *N. konggordous* sp. nov. is restricted to the Mamagou Grand Canyon on the southern slopes of the Himalayas, representing another case of allopatric speciation. Finally, *N. minor* sp. nov. was found in

the Qionglai Mountains. It has a much smaller distribution range than *N. irene*, which is widely distributed across the Hengduan Mountains. In some regions (e.g., Jiajin Mountain and Xiling Snow Mountain), the two species occur parapatrically, but *N. minor* sp. nov. occupies higher elevations (3,400–4,300 m) compared to *N. irene* (2,500–3,400 m). We hypothesize that climate and habitat differences are the drivers of divergence between *N. minor* sp. nov. and *N. irene*. The smaller body size of *N. minor* sp. nov. compared to *N. irene* may be an adaptation to its living at higher elevations.

Our study demonstrates that species diversity within the genus *Neodon* remains underestimated. Given the contiguous forest habitats in this region that span international boundaries, *N. konggordous* sp. nov. and *N. kulakangria* sp. nov. may also occur on the southern slopes of the Himalayas in neighboring areas of India. Owing to the large extent and complex topography of the southern slopes of the Himalayas, further strengthening of the biodiversity surveys in the region is likely to discover overlooked biodiversity, which will enhance the region's value.

Acknowledgments

This research was supported by the National Animal Collection Resource Center, China, and the Kunming Natural History Museum of Zoology, KIZ, CAS. This research was funded by the National Natural Science Foundation of China (NSFC 32370496), the Survey of Wildlife Resources in Key Areas of Tibet (ZL202203601), and the Huanglong Nature Reserve Comprehensive Scientific Investigation Report Preparation Project (N5132112023000495).

References

Allen G (1940) Mammals of China and Mongolia. Natural history of central Asia. American Museum of Natural History, New York.

Baker RJ, Bradley RD (2006) Speciation in mammals and the genetic species concept. Journal of Mammalogy 87(4): 643–662. https://doi.org/10.1644/06-MAMM-F-038R2.1

Chen ZZ, He SW, Hu WH, Song WY, Onditi KO, Li X-Y, Jiang X-L (2021) Morphology and phylogeny of scalopine moles (Eulipotyphla: Talpidae: Scalopini) from the eastern Himalayas, with descriptions of a new genus and species. Zoological Journal of the Linnean Society 193(2): 432–444. https://doi.org/10.1093/zoolinnean/zlaa172

Chen ZZ, Pei XX, Hu JX, Song WY, Khanal L, Li Q, Jiang XL (2024) Multilocus phylogeny and morphological analyses illuminate overlooked diversity of *Soriculus* (Mammalia: Eulipotyphla: Soricidae), with descriptions of two new endemic species from the eastern Himalayas. Zoological Journal of the Linnean Society 201(2): 534–548. https://doi.org/10.1093/zoolinnean/zlad131

Cheng F, He K, Chen ZZ, Zhang B, Wan T, Li JT, Zhang BW, Jiang XL (2017) Phylogeny and systematic revision of the genus *Typhlomys* (Rodentia, Platacanthomyidae), with description of a new species. Journal of Mammalogy 98: 731–743. https://doi.org/10.1093/jmammal/gyx016

Darriba D, Taboada G, Doallo R, Posada D (2012) jModelTest 2: More models, new heuristics and parallel computing. Nature Methods 9(8): 772. https://doi.org/10.1038/nmeth.2109

Ellerman JR (1941) The Families and Genera of Living Rodents. British Museum (Natural History), London.

Ellerman JR, Morrison-Scott TCS (1951) Checklist of Palaearctic and Indian mammals 1758 to 1946. British Museum (Natural History), London.

Galewski T, Tilak M, Sanchez S, Chevret P, Paradis E, Douzery EJP (2006) The evolutionary radiation of Arvicolinae rodents (voles and lemmings): Relative contribution of nuclear and mitochondrial DNA phylogenies. BMC Evolutionary Biology 6(1): 1–17. https://doi.org/10.1186/1471-2148-6-80

Ge DY, Feijó A, Abramov AV, Wen ZX, Liu ZJ, Cheng JL, Xia L, Lu L, Yang QS (2021) Molecular phylogeny and morphological diversity of the *Niviventer fulvescens* species complex with emphasis on species from China. Zoological Journal of the Linnean Society 191(2): 528–547. https://doi.org/10.1093/zoolinnean/zlaa040

He K, Li YJ, Brandley MC, Lin LK, Wang YX, Zhang YP, Jiang XL (2010) A multi-locus phylogeny of Nectogalini shrews and influences of the paleoclimate on speciation and evolution. Molecular Phylogenetics and Evolution 56(2): 734–746. https://doi.org/10.1016/j.ympev.2010.03.039

He K, Shinohara A, Helgen KM, Springer MS, Jiang XL, Campbell KL (2017) Talpid mole phylogeny unites shrew moles and illuminates overlooked cryptic species diversity. Molecular Biology and Evolution 34(1): 78–87. https://doi.org/10.1093/molbev/msw221

Heled J, Drummond AJ (2010) Bayesian inference of species trees from multilocus data. Molecular Biology and Evolution 27(3): 570–580. https://doi.org/10.1093/molbev/msp274

Hinton MA (1923) XII.—On the voles collected by Mr. G. Forrest in Yunnan; with remarks upon the genera *Eothenomys* and *Neodon* and upon their allies. Annals & Magazine of Natural History 11(61): 145–162. https://doi.org/10.1080/00222932308632833

Hinton MAC (1926) Monograph of the voles & lemmings (Microtinae) living and extinct. Vol. 1, Trustees of the British museum, London. https://doi.org/10.5962/bhl.title.8319

Hooper ET (1958) The male phallus in mice of the genus *Peromyscus*. Miscellaneous Publications (University of Michigan. Museum of Zoology) 105: 1–24. https://doi.org/10.3998/mpub.12946894

Hooper ET, Musser GG (1964) The glans penis in *Neotropical cricetines* (family Muridae) with comments on classification of muroid rodents. Miscellaneous Publications (University of Michigan. Museum of Zoology) 123: 1–57.

Horsfield T (1849) XX.—Brief notice of several mammalia and birds discovered by BH Hodgson, Esq., in Upper India. Annals and Magazine of Natural History 3: 202–203. https://doi.org/10.1080/03745485909494621

Huelsenbeck JP, Hillis DM (1993) Success of phylogenetic methods in the four-taxon case. Systematic Biology 42: 247–264. https://doi.org/10.1093/sysbio/42.3.247

Kimura M (1980) A simple method for estimating evolutionary rates of base substitutions through comparative studies of nucleotide sequences. Journal of Molecular Evolution 16(2): 111–120. https://doi.org/10.1007/BF01731581

Leaché AD, Reeder TW (2002) Molecular systematics of the Eastern Fence Lizard (Sceloporus undulatus): A comparison of Parsimony, Likelihood, and Bayesian approaches. Systematic Biology 51(1): 44–68. https://doi.org/10.1080/106351502753475871

Lidicker Jr WZ (1968) A phylogeny of New Guinea rodent genera based on phallic morphology. Journal of Mammalogy 49(4): 609–643. https://doi.org/10.2307/1378724

Liu SY, Sun ZY, Liu Y, Wang H, Guo P, Murphy RW (2012) A new vole from Xizang, China and the molecular phylogeny of the genus

Neodon (Cricetidae: Arvicolinae). Zootaxa 3235(1): 1–22. https://doi.org/10.11646/zootaxa.3235.1.1

Liu SY, Jin W, Liu Y, Murphy RW, Lv B, Hao HB, Liao R, Sun ZY, Tang MK, Chen WC, Fu JR (2017) Taxonomic position of Chinese voles of the tribe Arvicolini and the description of 2 new species from Xizang, China. Journal of Mammalogy 98: 166–182. https://doi.org/10.1093/jmammal/gyw170

Liu SY, Zhou CR, Meng GL, Wan T, Tang MK, Yang CT, Murphy RW, Fan ZX, Liu Y, Zeng T, Zhao Y, Liu SL (2022) Evolution and diversification of Mountain voles (Rodentia: Cricetidae). Communications Biology 5(1): 1417. https://doi.org/10.1038/s42003-022-04371-z

Luo AR, Qiao HJ, Zhang YZ, Shi WF, Ho SYW, Xu WJ, Zhang AB, Zhu CD (2010) Performance of criteria for selecting evolutionary models in phylogenetics: A comprehensive study based on simulated datasets. BMC Evolutionary Biology 10(1): 242. https://doi.org/10.1186/1471-2148-10-242

Matocq MD, Shurtliff QR, Feldman CR (2007) Phylogenetics of the woodrat genus *Neotoma* (Rodentia: Muridae): Implications for the evolution of phenotypic variation in male external genitalia. Molecular Phylogenetics and Evolution 42(3): 637–652. https://doi.org/10.1016/j.ympev.2006.08.011

Meredith RW, Janecka JE, Gatesy J, Ryder OA, Fisher CA, Teeling EC, Goodbla A, Eizirik E, Simao TL, Stadler T, Rabosky DL, Honeycutt RL, Flynn JJ, Ingram CM, Steiner C, Williams TL, Robinson TJ, Burk-Herrick A, Westerman M, Ayoub NA, Springer MS, Murphy WJ (2011) Impacts of the Cretaceous Terrestrial Revolution and KPg extinction on mammal diversification. science 334: 521–524. https://doi.org/10.1126/science.1211028

Miller MA, Pfeiffer W, Schwartz T (2010) Creating the CIPRES Science Gateway for inference of large phylogenetic trees. In: 2010 gateway computing environments workshop (GCE). IEEE, 1–8. https://doi.org/10.1109/GCE.2010.5676129

Patterson BD, Thaeler Jr CS (1982) The mammalian baculum: Hypotheses on the nature of bacular variability. Journal of Mammalogy 63(1): 1–15. https://doi.org/10.2307/1380665

Pradhan N, Sharma AN, Sherchan AM, Chhetri S, Shrestha P, Kilpatrick CW (2019) Further assessment of the Genus *Neodon* and the description of a new species from Nepal. PLoS ONE 14(7): e0219157. https://doi.org/10.1371/journal.pone.0219157

Puillandre N, Lambert A, Brouillet S, Achaz G (2012) ABGD, Automatic Barcode Gap Discovery for primary species delimitation. Molecular Ecology 21(8): 1864–1877. https://doi.org/10.1111/j.1365-294X.2011.05239.x

Rannala B, Yang Z (2013) Improved reversible jump algorithms for Bayesian species delimitation. Genetics 194(1): 245–253. https://doi.org/10.1534/genetics.112.149039

Ronquist F, Huelsenbeck JP (2003) MrBayes 3: Bayesian phylogenetic inference under mixed models. Bioinformatics19(12): 1572–1574. https://doi.org/10.1093/bioinformatics/btg180

Sikes RS, Animal C (2016) Guidelines of the American Society of Mammalogists for the use of wild mammals in research and education. Journal of Mammalogy 97(3): 663–688. https://doi.org/10.1093/jmammal/gyw078

Stamatakis A, Hoover P, Rougemont J (2008) A rapid bootstrap algorithm for the RAxML Web servers. Systematic Biology 57(5): 758–771. https://doi.org/10.1080/10635150802429642

State Council Decree (1992) Wildlife protective enforcement regulation of The People's Republic of China. The Ministry of Forestry of PR China. [In Chinese]

Sullivan RM, Calhoun SW, Greenbaum IF (1990) Geographic variation in genital morphology among insular and mainland populations of *Peromyscus maniculatus* and *Peromyscus oreas*. Journal of Mammalogy 71(1): 48–58. https://doi.org/10.2307/1381315

Tamura K, Stecher G, Kumar S (2021) MEGA11: Molecular evolutionary genetics analysis version 11. Molecular Biology and Evolution 38(7): 3022–3027. https://doi.org/10.1093/molbev/msab120

Teeling EC, Scally M, Kao DJ, Romagnoli ML, Springer MS, Stanhope MJ (2000) Molecular evidence regarding the origin of echolocation and flight in bats. Nature 403(6766): 188–192. https://doi.org/10.1038/35003188

Wilson DE, Reeder DM (1993) Mammal species of the world: a taxonomic and geographic reference, Second ed. Smithsonian Institution Press, Washington.

Wilson DE, Reeder DM (2005) Mammal species of the world: a taxonomic and geographic reference, Third ed. The Johns Hopkins Press, Baltimore.

Wu YD, Dai GD, Li L, Littlewood DTJ, Ohiolei JA, Zhang LS, Guo AM, Wu YT, Ni XW, Shumuye NA, Li WH, Zhang NZ, Fu BQ, Fu Y, Yan HB, Jia WZ (2022) Expansion of Cyclophyllidea biodiversity in rodents of Qinghai-Tibet plateau and the "out of Qinghai-Tibet plateau" hypothesis of Cyclophyllideans. Frontiers in Microbiology 13: 747484. https://doi.org/10.3389/fmicb.2022.747484

Yang Z, Rannala B (2010) Bayesian species delimitation using multilocus sequence data. Proceedings of the National Academy of Sciences of the United States of America 107(20): 9264–9269. https://doi.org/10.1073/pnas.0913022107

Yang Z, Rannala B (2014) Unguided species delimitation using DNA sequence data from multiple loci. Molecular Biology and Evolution 31(12): 3125–3135. https://doi.org/10.1093/molbev/msu279

Zhao XX, Li B, Lin GH, Ma WJ, Ju HL, Su JP, Zhang TZ (2017) Molecular identification of voles in the east of the Qinghai-Tibet Plateau. Acta Theriologica Sinica 37: 44–52. https://doi.org/10.16829/j.slxb.201701002

Supplementary material 1

Supplementary information

Authors: Xuming Wang, Xuan Pan, Yingxun Liu, Robert W. Murphy, Buqing Peng, Chao Duan, Rui Liao, Xin Wang, Shaoying Liu

Data type: docx

Link: https://doi.org/10.3897/zse.101.140898.suppl1